INVERSION OF EDDY CURRENT DATA USING HOLOGRAPHIC PRINCIPLES

B.P. Hildebrand and G.L. Fitzpatrick

Sigma Research, Inc.
Seattle Laboratory
565 Industry Drive
Seattle, WA 98188

INTRODUCTION

It has proven possible to convert eddy current data associated with flaws to images of these flaws using holographic principles [2,3] because electromagnetic waves propagate in metals [1] and because these waves have subsonic velocities at eddy current frequencies. The purpose of this paper is to review and clarify the physical and mathematical basis for this method of analyzing eddy current data.

The flow of electric currents, and the propagation of electromagnetic waves in classical materials (quantum effects are assumed to be unimportant) is governed by Maxwell's equations [1,4]. Prior to Maxwell the laws of electricity and magnetism could have been written as [4]

Coulomb's Law: $$\nabla \cdot \bar{D} = 4\pi\rho \tag{1}$$

Ampere's Law: $$\nabla \times \bar{H} = \frac{4\pi}{c} \bar{J} \tag{2}$$

Faraday's Law: $$\nabla \times \bar{E} = -\frac{1}{c} \frac{\partial \bar{B}}{\partial t} \tag{3}$$

The absence of magnetic poles: $$\nabla \cdot \bar{B} = 0 \tag{4}$$

In addition there are two constituitive relations for linear (nonferromagnetic) isotropic conductors $\bar{D} = \varepsilon\bar{E}$ and $\bar{B} = \mu\bar{H}$ where

$\bar{E}$ = electric field in free space
$\bar{H}$ = magnetic field in free space
$\bar{D}$ = electric displacement in matter
$\bar{B}$ = magnetic field in matter
$\bar{J}$ = electric current density
ρ = charge density
ε = electric permittivity (isotropic matter)
μ = magnetic permeability (isotropic matter)
c = free space light velocity.

Equations (1) through (4) imply that $\bar{E}$ and $\bar{B}$ or $\bar{H}$ are related and are capable of variation in time. However, Eqs. (1) through (4) are mathematically and physically inconsistent [1,4]. From Eq. (2)

$$\nabla \cdot (\nabla \times \bar{H}) = \frac{4\pi}{c} \nabla \cdot \bar{J} = 0 \tag{5}$$

or

$$\nabla \cdot \bar{J} = 0 \tag{6}$$

Equation (6) is clearly not consistent with the continuity equation

$$\nabla \cdot \bar{J} + \frac{\partial \rho}{\partial t} = 0 \tag{7}$$

which expresses the local conservation of electric charge and defines electric current. By making the replacement

$$\bar{J} \rightarrow \bar{J} + \frac{1}{4\pi} \frac{\partial \bar{D}}{\partial t} \tag{8}$$

in Eq. (2), Maxwell obtained what is now called the Maxwell-Ampere law

$$\nabla \times \bar{H} = \frac{4\pi}{c} \bar{J} + \frac{1}{c} \frac{\partial \bar{D}}{\partial t} \tag{9}$$

where $(1/4\pi)\partial\bar{D}/\partial t$ is the so-called displacement current density. This law (Eq. (9)) is now consistent with Eq. (7) since

$$\nabla \cdot \bar{J} + \frac{\partial \rho}{\partial t} = \nabla \cdot (\bar{J} + \frac{1}{4\pi} \frac{\partial \bar{D}}{\partial t}) = 0 \tag{10}$$

Maxwell's equations ((Eqs. 1,9,3,4)) predict that electromagnetic waves will propagate in free space, nonconducting matter, and in conductors [1,4].

ELECTROMAGNETIC WAVES IN CONDUCTORS

We have reviewed Maxwell's equations to remind the reader that the displacement current $(1/4\pi\ \partial\bar{D}/\partial t)$ is crucial for the existence of a physically sensible electromagnetic theory [1,4]. One of the predictions of this theory is that electromagnetic waves propagate even in good conductors [1] where $\bar{D} = \varepsilon\bar{E}$ and $\partial\bar{D}/\partial t$ are very small owing to the small value of ε in conductors. For example in copper with $\varepsilon \simeq 8.9 \cdot 10^{-12}$ (farad meter)$^{-1}$ and conductivity $\sigma \simeq 5.8 \cdot 10^{7}$ (ohm-meter)$^{-1}$, the conduction current density

$$\bar{J} = \sigma\bar{E} \tag{11}$$

is much larger than the displacement current. As a practical matter this means that in applications such as the calculation of eddy current densities [5], Eq. (2) can be used as an excellent first approximation to Eq. (9).

Refractive Indices of Conductors

Maxwell's equations predict that the real and imaginary parts of the refractive indices in a conductor at low frequencies are equal and

given by [1]

$$n(R) = n(I) = n = \sqrt{\frac{\sigma}{2\varepsilon\omega}} = \frac{c}{v} \tag{12}$$

Hence, ε must not be assumed to be identically zero because that would imply that electromagnetic waves do not propagate ($v = 0$). Since ε and v are small, but nonzero in conductors, the corresponding wavelengths can be comparable to the size of flaws. For example in copper at a typical eddy current frequency of $f = \omega/2\pi = 50$ KHz, we find $n \simeq 3.2 \cdot 10^6$, $v \simeq 93.4$ m/sec and $\lambda \simeq .19$ cm. Small wavelengths immediately open the possibility of imaging flaws using techniques such as computer assisted holography.

Observers Inside the Conductors

The imaginary part of the index of refraction is responsible for the attenuation of electromagnetic waves in conductors. Thus, the depth of penetration $z = \delta$ (skin depth) is defined to be the depth at which the wave amplitude, which experiences an attenuation $\beta = \omega n_i/c$, drops by 1/e. That is,

$$\exp(-\beta z) = 1 \tag{13}$$

and

$$z = \delta = \frac{v}{\omega} = \frac{\lambda}{2\pi} \cdot \tag{14}$$

For copper at 50 KHz, $\delta = \lambda/2\pi = .03$ cm. In the following discussion the observers inside the conductor are always assumed to be at a depth comparable to δ or less than δ. Given the refractive indices n_i and n_o (see Fig. 1), Snell's law yields the relation

$$\frac{\sin \phi_i}{c} = \frac{\sin \phi_r}{v_i} = \frac{n_i}{c} \sin \phi r \tag{15}$$

Since $v_i \ll c$ and ϕ_r is very small, an observer looking at S from inside the conductor looks toward a direction approximately normal to its surface. Thus,

$$\sin \phi_i \simeq x/h \tag{16}$$

$$\sin \phi_r \simeq x/h' \tag{17}$$

where h is the actual coil "liftoff". Consequently, h' is the apparent liftoff seen internally by the observer. Then combining Eq. (15) (16) (17), we have the apparent coil liftoff

$$h' \simeq n_i \, h \tag{17}$$

For h = 1mm over copper at f = 50 KHz, we have $h' \simeq 3.2 \cdot 10^3$ m. In summary the conductor (copper in this case) appears to an internal observer to be illuminated by a plane electromagnetic wave of wavelength $\lambda = v/f = .19$ cm, which is essentially parallel to the conductor surface owing to the great apparent distance of the eddy current coil (source) above the conductor.

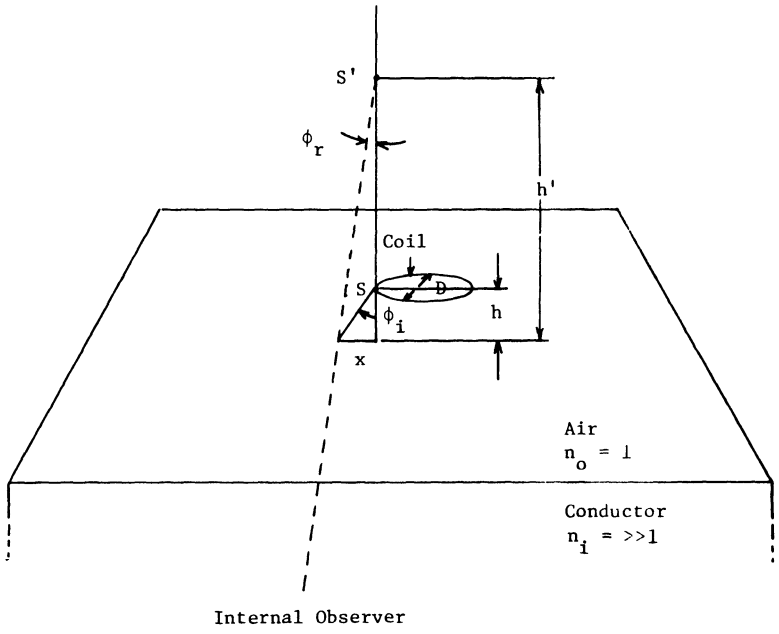

Fig. 1. A point S on an eddy current coil of diameter D as seen by observer located inside the conductor.

Phase Information

The internal observer at $(x,y,z<<\delta)$ sees the phase of the electromagnetic wave at the coil as $\theta(x,y)$ plus or minus some constant phase factor (due to liftoff) for all (x,y) [3,6]. If the corrected coil impedence is

$$Z(x,y) = R(x,y) + i\, I(x,y) \tag{18}$$

then

$$\theta(x,y) = \tan^{-1} \frac{I(x,y)}{R(x,y)} \tag{19}$$

and

$$\theta(x,y,z<<\delta) \propto \theta(x,y) \tag{20}$$

In summary, the phase $\theta(x,y,z<<\delta)$ measured at a point very near the conductor surface is responsive to a volume of the conductor together with any flaws within a skin depth δ. Thus $\theta(x,y,z<<\delta)$ contains distributed information from an aerial extent of the conductor even though it is measured at only one point $(x,y,z<<\delta)$.

EDDY CURRENT HOLOGRAPHY

For the foregoing reasons, let us consider the back propagation (holographic reconstruction) of this phase information. We will start with the spatial frequency components of the plane wave hologram at points very near the conductor surface $(x,y,z<<\delta)$ and propagate each of these back to a flaw location to produce an eddy current flaw image.

However, it should be stressed, that while the near surface phase information $\theta(x,y,z<<\delta)$ is consistent with a plane wave hologram, the amplitude response of the eddy current coil is dependent on coil size, flaw size and the distance from the flaw. The maximum amplitude response of an eddy current coil occurs in those regions where the eddy current densities are highest, namely just below the coil and within a skin depth δ of the conductor surface. Thus, the holographic information will also be amplitude modulated by coil-flaw-scan aperture geometric effects described by a function $g(x,y,z)$.

The procedure for reconstructing a plane wave eddy current, or other hologram (such as an acoustic hologram) described by the function

$$f(x,y,z) = g(x,y,z) \exp (j\theta(x,y,z)) \tag{21}$$

where

$$g(x,y,z) = \text{amplitude modulation} \tag{22}$$

is as follows [3].

1. Compute the two dimensional Fourier spatial transform of the hologram $f(x,y,z)$.

2. Multiply each spatial frequency component (plane wave) described by the wave numbers u,v by the complex wave propagation factor

$$\exp\{-\frac{2\pi j}{\lambda} [1 - (\lambda u)^2 - (\lambda v)^2]^{1/2} (z' - z)\} \tag{23}$$

3. Compute the inverse two-dimensional Fourier spatial transform of the result of (2) yielding the complex "hologram" information at the new depth of interest $f(x,y,z = z')$.

4. Use this back propagated holographic information to form an image of the flaw at depth $z = z'$ by computing and plotting a two-dimensional image $I = |f(x,y,z = z')|^2$

EXPERIMENTAL RESULTS

The reconstruction algorithm we employ operates best on holograms where there are a large number of fringes within the hologram aperture. There is an appreciable signal only where $g(x,y,z<<\delta)$ is different from zero. This region is the effective hologram aperture. In order to ensure that there are a sufficient number of such fringes in this region, we multiply $\theta(x,y,z<<\delta)$ by a factor K (ranging from K = 10 to about 40) before actual reconstructions are performed [3]. It is important to stress that this procedure does not add information, nor is it a fundamental requirement of eddy current imaging by holography.

We are currently pursuing the development of algorithms which would not involve K. These algorithms would essentially operate on the holographic information stored as gray values in the effective hologram aperture, rather than on fringes. However, for our purposes we will employ K - dependent algorithms, but keep in mind that this artifice may eventually be eliminated from the reconstruction procedure.

The basic reconstruction process as described in steps 1 through 4 can be put to a crucial experimental test by choosing an object (flaw) with a broad spatial frequency spectrum and by demonstrating that a proper flaw image results. Artificial targets, which possess such a spectrum, are square flat-bottomed holes as shown in Fig. (2). The high curvature of the corners of these holes and their sharp edges must be characterized by higher spatial frequencies. Clearly, these must be correctly propagated from the data plane $z<<\delta$ to produce a correct image at the image plane $z = z'$.

The two 1/2 in. x 1/2 in. square holes of Fig. (2) at two different depths from the surface ((.015 in., .050 in.)) were scanned in the manner illustrated in Fig. (3). Using a 1 in. diameter coil, the 1/2 in. x 1/2 in. hole at .050 in. depth produced the holographic data $f(x,y,z<<\delta)$ shown in Fig. (4a). Note that the range of coil "sensitivity" (S in Fig. (3)) and the scan pattern combine to produce an annular region Fig. (4a) where $g(x,y,z<<\delta)$ is appreciable. When a smaller 1/2 in. diameter coil is used to scan a similar target at .015 in (Fig. (2)), the central region of the annular region is filled in. The region where $g(x,y,z<<\delta)$ is appreciable is now circular in shape.

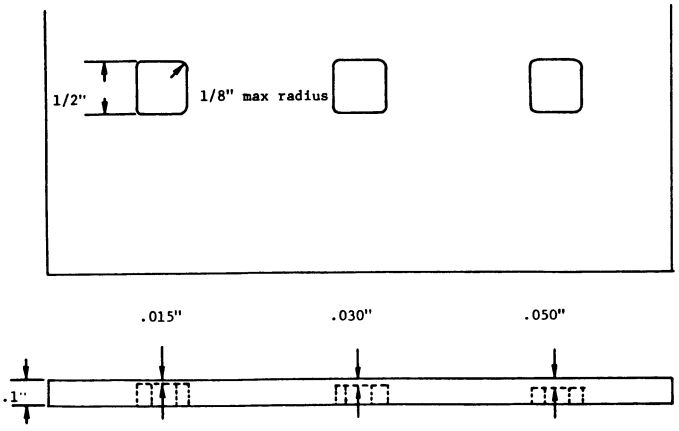

Fig. 2. Square flat-bottomed holes milled in 304-L stainless steel plate are illustrated. Coils of 1/2 in. and 1 in. diameter were used to scan the 1/2 in. x 1/2 in. holes in a 5 cm x 5 cm scan pattern as shown in Fig. (3).

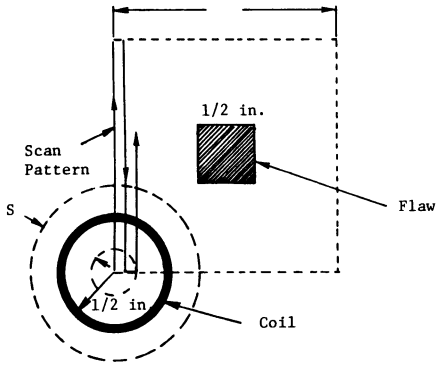

Fig. 3. Typical symmetric scan pattern for a circular coil.

CONCLUSIONS

Owing to the extremely low velocity of electromagnetic waves in conductors at eddy current frequencies (relative to the free space velocity of light), eddy current coils appear to observers located just inside these conductors to be point sources at "infinity". Thus the spatially modulated coil impedance phase, corrected for liftoff errors, can be used as a measure of the phase of the combined electromagnetic waves (from the conductor) interacting with the coil.

Holograms created using this phase information appear to have been made with a plane wave (point source at "infinity"), and these are easily reconstructed or back propagated to form images. To successfully perform such a reconstruction, it is necessary to assume that the spatial frequency content of the image (or target) can be propagated in a wave-like fashion from the image or object plane at depth $z = z'$ to the hologram plane and vise versa. This may be accomplished using standard phase propagation factors, where the propagation phase is that corresponding to the electromagnetic wave spatial frequency component to be propagated in some direction in the conductor.

A crucial experiment testing these ideas was performed. Square flat-bottomed holes in 304-L stainless steel were scanned with eddy current coils of two different diameters and the resultant holograms were reconstructed to produce successful images of these square holes. If the spatial frequency information content of the hologram had been incorrect, or if the backward wave propagation procedure had been physically invalid, the reconstruction algorithm could not have produced these correct images. We take this fact to be significant experimental confirmation of the inversion of eddy current data by holographic means.

Experimental evidence regarding the focusing characteristics of the eddy current data ($f(x,y,z<<\delta)$) is illustrated in Fig. (4). It is clear that the unfocused data shows no tendency whatever to have a square shape in either scan (4a) or (4c). However, the holographic reconstructions $|f(x,y,z = z')|^2$ do possess corners and edges as true focused images must. Moreover, if the scan direction is changed (not shown) to a diagonal scan, the images of these squares rotate by 45 degrees as one would expect of optical analog data. These observations mean that the spatial frequency content of the holographic data at the conductor surface is being properly propagated to the image plane $z = z'$. Therefore, true focusing in the optical sense is occuring.

It should be stressed that a true focused image (a square) results only when the correct velocity of propagation in 304-L stainless steel ($v = 240$ m/sec at 50 KHz) is used in the reconstruction process. Varying this velocity away from 240 m/sec, defocuses the image. Thus in a sense we can measure the velocity of propagation by observing when an image of known shape is properly focused. The value of 240 m/sec was also measured independently by noting the phase shift experienced by the 50 KHz wave in passing through a known thickness of material. This value was found to agree with the value required for focusing to occur. These facts provide additional evidence that we are not only dealing with electromagnetic waves, but that they are indeed being properly focused.

Note that the pattern of dark spots and the dark ring in Fig. (4b) are artifacts related to the annular shape of the effective hologram aperture of Fig. (4a). Similar spots are seen in Fig. (4d) and are due to a similar diffraction pattern produced by the effective hologram aperture of Fig. (4c).

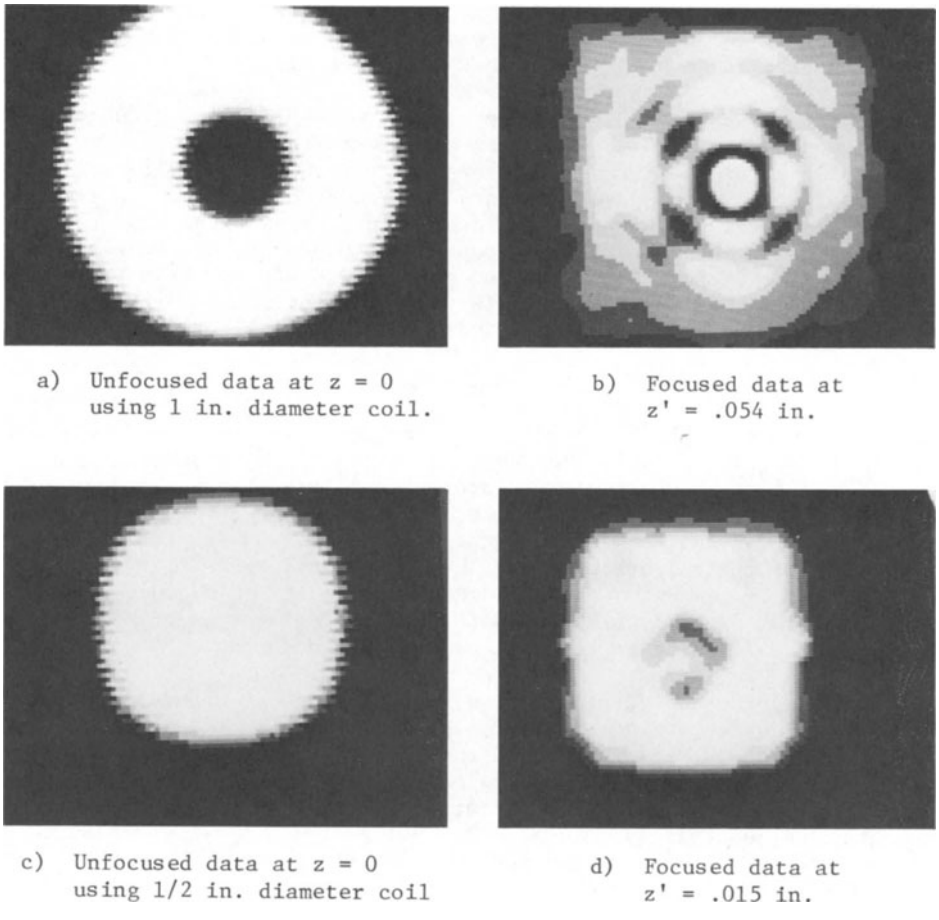

a) Unfocused data at z = 0 using 1 in. diameter coil.

b) Focused data at z' = .054 in.

c) Unfocused data at z = 0 using 1/2 in. diameter coil

d) Focused data at z' = .015 in.

Fig. 4. Hologram data $f(x,y,z<<\delta)$ and reconstructed images $|f(x,y,z = z')|^2$ of square holes (see Fig. (2)) in 304-L stainless steel.

REFERENCES

1. R.P. Feynman et al., The Feynman Lectures on Physics, Vol. II Addison Wesley, Massachusetts (1964). (Ch. 18,32 are particularly relevant).
2. H.D. Collins, T.J. Davis, L.J. Busse et al., "Eddy Current Phasography," in Acoustical Imaging, Vol. 11, edited by John P. Powers, Plenum Press, New York, pp. 609-623.(1982)
3. B.P. Hildebrand, A.J. Boland, T.J. Davis, "Holographic Principles Applied to low Frequency Electromagnetic Imaging in Conductors," in IEEE proceedings of The 10th International Optical Computing Conference, IEEE Computer Society Press, (1983).
4. J.D. Jackson, Classical Electrodynamics, John Wiley & Sons, New York, (1965). (See p. 177)
5. W. Lord, "Development of a Finite Element Model for Eddy Current NDT Phenomena," Electric Power Research Institute Report #EPRI NP-2026 (1981).
6. In practice, information from a reference coil operating at 200 KHz well above the conductor surface and a 200 KHz signal on the probe coil near the surface are used to correct for liftoff errors. These are phase errors introduced into the 50 KHz probe signal due to variations in distance from the conductor surface. For a further discussion of this process see reference 3.